International Journal of Research in Engineering and Innovation Vol-10, Issue-5 (2026), 185-195

International Journal of Research in Engineering and Innovation (IJREI)

Journal home page: https://ijrei.com/

REVIEW PAPER

Wire arc additive manufacturing of Inconel 625: A review

Amit Kumar Punia[1*], Rakesh Kumar[1], Arvind Jayant[2]

[1]*Department of Mechanical Engineering, Sant Longowal Institute of Engineering and Technology (SLIET), Longowal–148106, Punjab, India*
[2]*Department of Mechanical Engineering, Indira Gandhi Delhi Technical University for Women (IGDTUW), New Delhi*

Article Information

Received: 21 July 2026
Revised: 19 August 2026
Accepted: 01 September 2026
Available online: 03 September 2026

Keywords:

Inconel 625
Wire arc additive manufacturing
Directed energy deposition
Cold metal transfer
Heat treatment
Microstructure
Mechanical anisotropy
Corrosion
Thermal history

Abstract

Wire arc additive manufacturing (WAAM) enables economical near-net-shape production of large Alloy 625 components, but repeated arc-heating cycles create location-dependent microstructures and properties. This critical narrative review synthesizes 2020–2026 evidence through a process–thermal history–microstructure–performance framework, emphasizing deposition mode, interpass control, segregation, defects, post-deposition heat treatment and mechanical/environmental response. The literature consistently reports a textured γ-Ni dendritic matrix with Nb–Mo enrichment and interdendritic constituents in the as-deposited condition. Low-heat-input, interrupted and field-assisted strategies can refine microstructure and improve selected tensile or wear outcomes, whereas uncontrolled heat accumulation increases heterogeneity. Solution treatment can dissolve Nb-rich constituents, while ageing may strengthen through precipitation; neither provides a universal benefit because grain growth, phase evolution and cooling route create competing effects. Cross-study comparison remains limited by inconsistent heat-input conventions, sparse thermal histories, non-uniform coupon extraction and insufficient fatigue, creep and service-environment data. The distinctive contribution is an evidence hierarchy, a condition-aware quantitative synthesis, an evidence-linked gap matrix and a minimum reporting framework for qualification-oriented research. Reliable WAAM Alloy 625 therefore requires control and reporting of the entire thermal trajectory rather than optimization of isolated welding parameters.

1. Introduction

Inconel 625 (IN625), also referred to generically in the literature as Alloy 625 (UNS N06625; INCONEL® is a registered trademark of Special Metals Corporation), is a solid-solution-strengthened Ni–Cr–Mo–Nb alloy selected for aggressive marine, chemical, energy and aerospace environments because it combines weldability, corrosion resistance and useful strength over a broad temperature range. Conventional manufacture of large IN625 parts commonly entails high material cost, low machinability and a large buy-to-fly ratio. WAAM addresses these constraints by coupling wire feedstock with an electric arc and numerically controlled motion to build near-net-shape components at deposition rates substantially above powder-bed systems. The trade-off is a comparatively coarse surface, lower geometric resolution and a strongly history-dependent thermal field.

Between 2020 and 2026, research moved beyond feasibility demonstrations toward control of droplet transfer, discontinuous CMT, torch-path planning, post-deposition heat treatment, environmental performance, bimetallic architectures and predictive modelling. The central scientific problem is nevertheless unchanged: each new layer reheats earlier material, so the final wall is a stack of locally different solidification and tempering histories. Consequently, chemistry alone does not determine performance. Heat input, interpass temperature, deposition direction, wire diameter, wall geometry, shielding, dwell time and post-processing

Corresponding author: Amit Kumar Punia
Email Address: ipoonia@gmail.com
https://doi.org/10.36037/IJREI.2026.10501

collectively govern grain morphology, texture, segregation, phase stability, residual stress and defect population [1–9].

This article critically reviews studies published during 2020–2026 and develops an experimentally actionable synthesis for future work on GMAW/CMT-fabricated IN625 walls. Unlike broad reviews of all WAAM alloys, it concentrates on the interaction between thermal management and the mechanical/metallurgical response of IN625. The main questions are: (i) which process variables most strongly determine bead stability and heat accumulation; (ii) how do repeated thermal cycles control phase formation and spatial heterogeneity; (iii) when do solution treatment and ageing improve or degrade performance; and (iv) what evidence is still needed for industrial qualification?

1.1 Positioning relative to earlier reviews

Earlier reviews have established the broad capabilities, defects and application landscape of WAAM and have summarized the microstructure and mechanical properties of arc-deposited Alloy 625 [9,21,31,33–35,40]. The present review differs in five respects: it confines the principal evidence synthesis to 2020–2026; treats the complete thermal trajectory as the organizing variable; integrates deposition mode with solution treatment, ageing and service-environment response; distinguishes direct Alloy 625 experiments from modelling, bimetallic and general-WAAM evidence; and converts the synthesis into minimum reporting and qualification requirements. Its intended contribution is therefore not another catalogue of WAAM parameters, but a critical explanation of why nominally similar Alloy 625 builds develops different phases and properties.

1.2 Research Questions

RQ1. How do arc mode, heat and mass input, path strategy and interpass control determine the thermal history of WAAM Alloy 625?

RQ2. How does thermal history govern grain morphology, segregation, defects, texture and secondary-phase formation?

RQ3. Under which starting conditions and temperature–time schedules do solution treatment and ageing improve mechanical and environmental performance?

RQ4. Which evidence gaps currently prevent reproducible comparison and industrial qualification?

RQ5. What minimum experimental and reporting framework is required for transferable process–thermal history–microstructure–performance relationships?

1.3 Contributions of this review

- A consolidated process–thermal history–microstructure–performance framework for Alloy 625 WAAM.
- A critical comparison of heat-treatment schedules and precipitation mechanisms rather than a simple paper-by-paper summary.
- A quantitative, condition-aware synthesis of selected tensile, hardness, wear and corrosion outcomes.
- An explicit evidence hierarchy separating direct experiments, modelling, bimetallic studies, reviews and specification sources.
- An evidence-linked research-gap matrix and a qualification-oriented reporting checklist.

2. Review Methodology and Scope

A critical narrative-review approach was adopted. Targeted searches were conducted for literature published from January 2020 to 3 August 2026 using Crossref-indexed publisher records and scholarly discovery services. Search combinations included Inconel 625 or Alloy 625 with wire arc additive manufacturing (WAAM), wire-arc directed energy deposition, CMT, GMAW, GTAW, heat treatment, microstructure, mechanical properties, corrosion, oxidation, wear, residual stress, thermal model and sustainability. Peer-reviewed studies directly addressing arc-deposited Alloy 625 were prioritized. Recent WAAM-wide reviews and one manufacturer datasheet were used only for mechanism or nominal-composition context and were not treated as direct experimental evidence. Because database coverage, indexing and experimental reporting were heterogeneous, this study is presented as a critical narrative review rather than a systematic review or meta-analysis.

Studies were retained when they reported the feedstock and arc-deposition route, a defined processing or post-treatment condition, and at least one microstructural, mechanical, corrosion, oxidation, wear, thermal or environmental outcome. Studies dominated by laser or powder-bed processes were excluded except where a phase-transformation mechanism was explicitly identified as contextual rather than direct WAAM evidence. Evidence was organized through a process–thermal history–microstructure–performance framework. Numerical results were compared only when the specimen condition, orientation, wall location and test temperature were sufficiently clear. The review therefore emphasizes mechanistic consistency, boundary conditions and research gaps instead of pooled effect sizes. Figure 1 illustrates the framework used to organize this evidence.

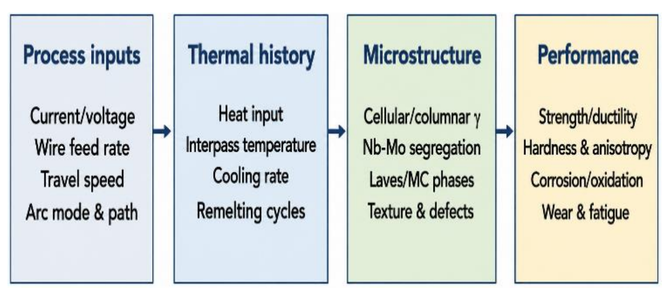

Figure 1: Process–thermal history–microstructure–performance framework used in this review (authors' synthesis).

2.1 Evidence classification and interpretation

The evidential weight assigned to a study depended on its relationship to monolithic arc-deposited Alloy 625. Direct experiments were used for material-specific conclusions; validated numerical studies supported thermal and residual-stress interpretation; bimetallic studies informed interface behavior only; general WAAM and review papers provided contextual mechanisms; and manufacturer/specification data supplied nominal chemistry rather than performance evidence. Table 1 summarises this evidence hierarchy.

Table 1: Evidence hierarchy used to interpret the 2020–2026 literature.

Evidence class	Permitted use in this review	Main limitation
Direct monolithic Alloy 625 experiment	Primary basis for process, microstructure and property conclusions	Platform, geometry and test-condition dependence
Validated thermal/mechanical model	Interpretation of temperature, stress and distortion fields	Dependent on boundary conditions and material inputs
Bimetallic/graded Alloy 625 study	Interface, dilution and deposition-order evidence	Not transferable to monolithic-wall bulk properties
General WAAM or Ni-superalloy review	Context, terminology and mechanism mapping	Secondary evidence; alloy specificity may be weak
Manufacturer/specification source	Nominal chemistry and wrought reference values	Not evidence of WAAM performance

3. Alloy Metallurgy Relevant to WAAM

3.1 Nominal chemistry and strengthening

IN625 contains a γ face-centred-cubic Ni matrix with Cr for oxidation/corrosion resistance and Mo plus Nb for solid-solution strengthening. In rapid arc solidification, partition coefficients cause Nb and Mo to enrich the interdendritic liquid. This promotes MC-type carbides and a Nb-rich Laves constituent when local solidification conditions and cumulative reheating permit. The same Nb reservoir can participate in metastable γ″ (Ni_3Nb) or orthorhombic δ precipitation during subsequent thermal exposure.

Table 2: Nominal composition range and metallurgical functions for Alloy 625 (UNS N06625); nominal limits are based on the manufacturer technical bulletin [28] and must be verified against the actual wire certificate before experimentation.

Element	Typical specification (wt.%)	Metallurgical role in WAAM IN625
Ni	≥58	γ-matrix; austenite stability
Cr	20–23	Passivation and oxidation resistance
Mo	8–10	Solid-solution strengthening; interdendritic segregation
Nb + Ta	3.15–4.15	Strengthening; Laves/MC/δ/γ″ formation
Fe	≤5	Balance/solid-solution constituent
C	≤0.10	MC and $M_{23}C_6$ carbide formation
Si, Mn, Al, Ti	controlled minor additions	Deoxidation and secondary-phase effects

The practical goal is not simply to maximize precipitate content: continuous or coarse interdendritic phases can reduce ductility and corrosion uniformity, whereas controlled fine precipitation may raise hardness or yield strength [1,4,10–12]. Table 2 summarises the nominal composition and metallurgical role of each element.

3.2 Spatially heterogeneous solidification

The bottom of a wall experiences rapid heat extraction into the substrate and generally exhibits finer cellular or columnar structures. As height increases, substrate influence diminishes, heat accumulates and the thermal gradient/cooling rate changes. Upper and central regions may therefore show coarser dendrites, altered secondary dendrite arm spacing and locally equiaxed grains. Epitaxial growth across fusion boundaries creates texture and contributes to direction-dependent tensile response. Alternating torch paths reduce systematic start–stop height errors but do not automatically eliminate microstructural anisotropy [2,3,6,13].

Thermal cycling also creates a distinction between the newly deposited top layers and reheated lower layers. Earlier layers may undergo partial homogenization, recovery or precipitation during the build, while the top retains a more recently solidified structure. Reporting only one micrograph or one hardness location can therefore conceal the dominant material gradient.

4. Processing Routes and Control Variables

4.1 Arc mode and metal transfer

GMAW-based WAAM provides high productivity and straightforward robotic integration. CMT lowers average heat input by controlled wire retraction and short-circuit transfer; pulsed and CMT-cycle-step/discontinuous modes further modify droplet frequency and cooling time. GTAW or hot-wire GTAW offers independent control of arc and wire but may reduce deposition rate. Recent comparisons show that transfer stability is not merely a geometric concern: it affects dilution, dendrite scale, defect population and electrochemical response [3,5,7,14,41].

Votruba et al. [5] reported that discontinuous CMT produced a finer, partly recrystallized structure and approximately 15% higher room-temperature UTS than continuous CMT, with roughly twofold better wear resistance at 650 °C. Such gains came at the cost of lower productivity and greater shielding-gas consumption. Hence, the preferable mode depends on whether thin-wall precision, throughput, gas use or elevated-temperature service is dominant.

4.2 Heat input, wire feed and travel speed

Nominal arc energy per unit length is commonly estimated from the measured voltage V, current I, travel speed v and process-efficiency factor η. When V is in volts, I in amperes and v in mm/min, the expression is $H = (\eta \times 60VI)/(1000v)$ kJ/mm. If travel speed is expressed in mm/s, the corresponding expression is $H = \eta VI/(1000v)$ kJ/mm. State the chosen efficiency factor and unit convention. This nominal value does not capture wire enthalpy, waveform-dependent metal transfer, dwell time, interpass temperature, geometry-dependent heat loss or reheating of earlier layers. Increasing wire feed generally raises deposition rate and bead cross-section; increasing travel speed reduces energy and deposited mass per unit length, but excessive speed risks lack of fusion and unstable continuity. Higher current can improve wetting while increasing penetration and accumulated heat. The relevant optimization target is therefore a stable thermal–mass-transfer window rather than a single minimum-heat setting [3,6,8,15].

4.3 Interpass temperature and path strategy

Interpass temperature is a state variable linking one layer to the next. Fixed dwell time is inadequate when wall height or ambient heat loss changes; temperature-triggered deposition is more reproducible. Bidirectional/reciprocating paths can balance start and end transients, while discontinuous or segmented deposition allows local cooling. Thick walls introduce overlap and remelting effects absent in single-bead walls.

Table 3: Mechanistic effects of principal WAAM variables for IN625.

Variable	Primary physical effect	Expected response when increased	Key risk / control need
Current/ voltage	Arc power and penetration	Wider bead, greater dilution and heat accumulation	Coarsening, distortion, substrate mixing
Wire-feed rate	Mass deposition and arc balance	Greater bead area/height within stable range	Stubbing or unstable transfer if unmatched
Travel speed	Energy and mass per unit length	Narrower bead; faster cooling	Lack of fusion or discontinuity
Interpass temperature	Initial condition of next layer	Lower cooling rate and more reheating	Vertical heterogeneity and grain coarsening
Dwell time	Cooling opportunity	Lower interpass temperature	Reduced productivity; not geometry-adaptive
Path direction	Heat-flow and start/stop distribution	Can balance wall height and residual stress	Directional texture persists
Shielding gas/ flow	Arc physics and oxidation protection	Improved protection up to effective coverage	Turbulence, entrainment and gas cost
Wire diameter	Current density, melting and bead scale	Changes deposition stability and hardness response	Requires re-optimized waveform and feed

Closed-loop control using infrared sensing, pyrometry, current/voltage logging and layer-height feedback is consequently more transferable than open-loop recipes [5,6,9,16]. Table 3 summarises the mechanistic effect of each principal process variable.

5. Microstructure, Defects and Residual Stress

5.1 Dendritic structure, segregation and secondary phases

Across the recent literature, the recurring as-deposited signature is a γ-Ni dendritic matrix with Nb/Mo-enriched interdendritic regions. Laves constituents, Nb/Ti-rich MC carbides and, after suitable thermal exposure, δ-Ni_3Nb, γ″ or grain-boundary carbides have been reported depending on thermal history and characterization resolution. These features matter because interconnected interdendritic constituents can provide crack-initiation paths, consume strengthening solute and create local electrochemical heterogeneity. Higher heat input generally enlarges dendritic spacing, whereas low-heat-input, interrupted or magnetically assisted strategies can refine the structure and reduce segregation [1–7,10,14,22].

Phase identification requires caution. Optical contrast or SEM morphology alone cannot unambiguously distinguish Nb-rich Laves constituents, MC/$M_{23}C_6$ carbides, δ-Ni_3Nb and nanoscale γ″. SEM–EDS can establish local elemental enrichment but cannot positively identify γ″. XRD is useful for the γ matrix and sufficiently abundant crystalline secondary phases, although low-volume-fraction nanoscale γ″ may remain below conventional detection limits. EBSD should be used principally for grain morphology, texture, misorientation and sufficiently coarse indexable phases. Confident identification of nanoscale γ″/δ precipitation requires TEM with diffraction and, where available, high-energy or synchrotron X-ray diffraction. Quantitative phase fraction, composition, secondary dendrite arm spacing and grain/texture data should be reported at bottom, middle and top wall locations [27].

Solidification may be interpreted through the temperature gradient G and interface growth rate R. A high G/R ratio favours columnar growth, whereas reduced G/R increases the tendency towards equiaxed grains; the cooling-rate-related product G×R influences dendrite scale. In multilayer WAAM these quantities evolve with height, local curvature and reheating, so a single 'cooling rate' cannot represent an entire wall. Secondary dendrite arm spacing should therefore be measured spatially and interpreted together with thermal-cycle descriptors rather than used as an isolated microstructural statistic [25,29,32].

The literature agrees that Nb and Mo enrich interdendritic liquid, but it does not support a universal monotonic relationship between heat input and final strength. Lower heat input commonly refines dendrites, yet strength also depends on dilution, porosity, texture, residual stress and subsequent precipitation. Likewise, dissolution of a brittle Nb-rich constituent may improve chemical homogeneity without increasing every tensile metric if simultaneous grain growth reduces boundary strengthening. These coupled effects explain apparently conflicting heat-treatment outcomes and should replace simple statements that 'finer grains' or 'less Laves phase' must always increase all properties [1,11,18,26,27,36]. Recent studies further broaden the process space through aerospace-oriented technology development, wire-diameter variation, data-driven tensile prediction and post-treatment erosion testing [12,16,37,39,42]. They reinforce the need to report machine-specific boundary conditions and to validate models outside the training or optimization dataset.

5.2 Defects and geometric integrity

Common risks include lack of fusion, porosity, oxide inclusions, start/stop irregularity, side-wall waviness, distortion and hot cracking. IN625 is weldable, but segregation and restraint can still create local crack susceptibility. X-ray computed tomography is valuable for volumetric defect mapping, while metallography alone may miss sparse three-dimensional porosity. Surface waviness must be separated from internal integrity because machining allowance can remove the former but not subsurface lack of fusion [5,13,17].

5.3 Residual stress and anisotropy

Steep thermal gradients and repeated restraint generate residual stress, while epitaxial grains and layer interfaces generate anisotropy. Tensile coupons extracted parallel and perpendicular to the build direction often show different yield, ultimate strength and elongation. However, cross-study comparison is weakened by non-uniform coupon geometry, unspecified extraction position and inconsistent surface preparation. A qualification-oriented study should map residual stress and hardness before coupon removal and test both orientations at multiple wall heights.

6. Post-Deposition Heat Treatment

6.1 Solution annealing

Solution annealing is intended to reduce chemical heterogeneity and dissolve Nb-rich interdendritic phases. Safarzade et al. [1] showed dissolution of Laves and δ constituents after solution treatment, accompanied by replacement of the dendritic appearance with large columnar grains. More recent CMT studies similarly report improved homogenization, but not every mechanical property increases simultaneously: grain growth can reduce strengthening, and cooling rate after solution treatment affects subsequent precipitation. Thus, "solution treated" is not a complete experimental condition; temperature, holding time, atmosphere, heating rate, cooling route and section thickness must be stated.

6.2 Ageing and precipitation

Ageing can generate γ'' and grain-boundary carbides, raising hardness or yield strength, but prolonged exposure may promote δ phase or coarse carbide networks and reduce ductility or corrosion resistance. The starting segregation state created during deposition determines the subsequent precipitation path. Time-based annealing at 980 °C for 30–120 min produced a modest UTS improvement, with the 2 h condition giving the best mechanical response in one CMT-WAAM study [26]. In-situ synchrotron diffraction has since shown that phase evolution during heat treatment is strongly schedule-dependent [27]. More recent arc-DED work proposed 1150 °C/4 h solution treatment followed by 650 °C ageing, with an optimized long ageing duration, illustrating that a wrought-alloy schedule cannot be transferred without microstructural and property validation [18].

6.3 Evidence-based heat-treatment matrix

Table 4 consolidates the purpose, likely benefit, potential risk and required verification for each heat-treatment condition.

Table 4: Heat-treatment logic for WAAM IN625; exact schedules must be experimentally validated rather than assumed.

Condition	Typical purpose	Likely beneficial change	Potential adverse change	Required verification
As-deposited	Baseline / avoid extra cost	Retention of fine dendrites and solid-solution strength	Segregation, Laves phase, residual stress	Spatial phase map; orientation-specific properties
Stress relief	Reduce residual stress	Dimensional stability	Unintended precipitation within sensitization range	XRD/SEM, residual stress, corrosion
Solution treatment	Homogenize and dissolve Laves/δ	Reduced segregation; improved phase uniformity	Grain growth; strength/ductility trade-off	EDS maps, grain size/texture, tensile
Direct ageing	Develop fine strengthening precipitates	Higher hardness/yield strength	δ/carbide coarsening; embrittlement	TEM/XRD, hardness map, toughness
Solution + ageing	Reset then control precipitation	More uniform response	Long cycle, energy cost, over-ageing	Full property and cost assessment

7. Mechanical and Environmental Performance

Cross-study mechanical comparison is complicated by coupon direction, extraction height, surface machining, gauge geometry, strain rate and heat-treatment nomenclature. Horizontal specimens may sample long columnar grains differently from vertical specimens, while machined coupons remove the rough surface that can dominate as-built fatigue initiation. Consequently, an apparent orientation effect cannot be attributed to crystallographic texture without also considering defects and specimen preparation. The most defensible comparisons are paired conditions fabricated on the same equipment, such as continuous versus discontinuous

CMT or field-assisted versus unassisted deposition [5,14,20,22,37,38].

7.1 Tensile properties, hardness and elevated temperature

Most recent studies report room-temperature tensile strength comparable with cast or specification minima, although values depend on direction, location, transfer mode and heat treatment. Low-heat-input discontinuous CMT improved UTS and retained properties more effectively at 650 °C than continuous CMT in one controlled comparison [5]. Hardness is typically moderate and spatially non-uniform; it reflects dendrite scale, solute distribution and precipitation rather than a simple top-to-bottom trend. Mechanical conclusions should therefore be supported by replicated coupons and statistical uncertainty.

Table 5: Quantitative outcomes reported in representative studies. Values are not pooled because process, orientation, wall location, heat treatment and test methods differ.

Study / condition	Process or treatment	Orientation /location	Reported tensile or hardness result	Other reported outcome	Comparability note
Tanvir et al. [26]	CMT-WAAM; 980 °C, 30–120 min, water quench	Thin wall; study-specific extraction	Approximately 5% UTS improvement; 2 h gave best reported mechanical response	YS rose after 2 h; hardness/strength linked to secondary phases	Relative result; consult source for absolute values and coupon geometry
Votruba et al. [5]	Discontinuous versus continuous CMT	Horizontal and vertical; 20 and 650 °C	Discontinuous CMT: ≈15% higher UTS at 20 °C and ≈4% better strength retention at 650 °C	Wear volume at 650 °C ≈ one-half of continuous CMT	Direct within-study comparison; lower productivity and higher gas use
Saravanakumar et al. [13]	Multi-layer WAAM wall	Bottom versus top zones	Average microhardness reported near 243.5 and 243.3 HV0.1; bottom zone showed higher UTS	Top-zone cracking reported in fractography	Small location-resolved dataset; process-specific
Yu et al. [22]	Static-magnetic-field-assisted WAAM	Horizontal / vertical	UTS 729/660 → 775/692 MPa; ≈6.3%/4.8 % improvement	Microhardness increased ≈6–7%; Nb/Mo segregation reduced	2026 direct comparison; verify exact test standard in source

Data remain sparse for fatigue, creep-fatigue interaction, fracture toughness and dwell-fatigue—properties central to aerospace and energy service. Static tensile adequacy cannot substitute for damage-tolerant qualification. Future experiments should relate crack initiation to defects, interdendritic constituents, build orientation and machined surface condition. Table 5 collates the quantitative outcomes reported for representative studies.

7.2 Corrosion and oxidation

Alloy 625 derives corrosion resistance from Cr-rich passivation and Mo-assisted resistance in chloride media. WAAM alters local chemistry through segregation, dilution and secondary-phase formation; droplet transfer and thermal history can therefore change pitting initiation even when bulk chemistry is nominally unchanged [4,10]. Evidence from WAAM Alloy 718 can clarify generic Ni-superalloy corrosion mechanisms but must not be treated as direct Alloy 625 property evidence. Quantitative comparison should report open-circuit stabilization, corrosion potential, corrosion-current density, pitting or breakdown potential and impedance-model parameters together with electrolyte composition, temperature, scan rate, exposed area and surface finish. Longer immersion, intergranular-corrosion and high-temperature oxidation exposures are needed to validate short electrochemical tests [10,12,19].

Environmental performance should be separated into general aqueous corrosion, pitting, intergranular attack, high-temperature oxidation and hot corrosion because each respond to different microstructural features. Cr-rich passive-film stability governs general corrosion; local Nb/Mo depletion and secondary phases may influence pitting or intergranular attack; oxide-scale adherence controls high-temperature oxidation; and molten salts introduce fluxing mechanisms not represented by room-temperature polarization. A single corrosion-current density therefore cannot validate marine, chemical and turbine service simultaneously [4,10,12,19,30,39].

7.3 Wear and machinability

Wear behavior becomes especially relevant where WAAM IN625 is used for repair, cladding or hot sliding contact. At elevated temperature, oxidation-assisted tribofilms can change the governing mechanism. The superior 650 °C wear resistance reported for discontinuous CMT illustrates that deposition strategy can have service-level consequences [5]. Near-net-shape parts nevertheless require machining; tool wear, residual stress redistribution and anisotropic cutting response should be considered in the total manufacturing route [17,20].

7.4 Sustainability and industrial relevance

A 2024 life-cycle comparison of an IN625 impeller found substantially lower energy use and material waste for WAAM than conventional machining, although results depend on system boundaries, deposition efficiency, machining allowance and electricity mix [8]. Discontinuous modes and long heat treatments may improve properties while increasing gas and energy consumption. Consequently, optimization should be multi-objective: deposition quality, final performance, buy-to-fly ratio, post-processing burden, energy and shielding-gas use should be assessed together.

8. Comparative Synthesis of 2020–2026 Studies

Table 6 critically compares representative studies published within the review window.

Table 6: Critical comparison of representative studies within the defined publication window.

Year / ref.	Process or focus	Principal contribution	Critical limitation / implication
2020 [1]	WAAM + solution/ageing	Established dissolution/precipitation and property trade-offs	Single material/process history; schedule transferability limited
2020 [2]	GMAW slab; as-built vs solution annealed	Demonstrated location-dependent microstructure and property change	Limited service-environment testing
2020 [3]	Thick wall; torch paths	Showed path-dependent surface quality and dendritic evolution	Thermal field not fully closed-loop controlled
2021 [4]	Droplet transfer	Linked transfer behavior to microstructure, mechanics and corrosion	Equipment-specific transfer regimes
2020 [7]	Super-TIG WAAM	Documented microstructural feasibility for IN625	Restricted parameter/property space
2021 [10]	Microstructure and intergranular corrosion	Connected microstructure with corrosion response	Limited long-duration exposure
2022 [5]	Continuous vs discontinuous CMT	15% room-temperature UTS gain and better hot wear for discontinuous CMT	Lower productivity and higher gas consumption
2022 [6]	WAAM microstructure/properties	Spatial characterization and property benchmarking	Needs broader fatigue/creep data
2022 [19]	High-temperature oxidation	Clarified oxidation performance of WAAM IN625	Specific atmosphere and thermal exposure
2023 [11]	CMT wall + post heat treatment	Compared metallurgical/mechanical response after treatment	Heat-treatment window still narrow
2023 [15]	Geometry and mechanical optimization	Used designed experiments to optimize bead/deposit response	Model validity constrained to studied platform
2023 [17]	Drillability of WAAM IN625	Quantified downstream machining behavior	Does not resolve deposition-property control
2024 [8]	LCA of IN625 impeller	Demonstrated potential energy/material advantage	Outcome sensitive to assumptions and post-processing
2024 [13]	Microstructure/mechanics by height	Confirmed bottom–top differences and top-zone cracking	Limited sample size and process breadth
2024 [16]	ANN tensile prediction	Demonstrated data-driven property prediction	Generalization needs larger, standardized datasets
2024 [21]	Focused review	Synthesized microstructure, mechanics and corrosion	Highlights same scarcity of orientation/corrosion data
2025 [12]	Post-treatment wear/corrosion	Extended evidence to high-temperature tribocorrosion	Long-term service validation still needed
2026 [18]	Long ageing of arc-DED IN625	Examined precipitation and property evolution after 650 °C/108 h	One ageing trajectory cannot define optimum
2026 [22]	Static-magnetic-field-assisted WAAM	Linked process to microstructure evolution and properties	Requires comparison with CMT/GMAW at matched heat input
2024 [23]	Thermo-mechanical simulation	Modelled transient thermal field and stress evolution	Needs extensive in-situ validation
2026 [24]	Bimetallic P22/IN625 WAAM	Demonstrated interface-specific microstructure/property correlations	Bimetallic result not directly transferable to monolithic walls
2026 [25]	Thermal-cycle experimental–numerical study	Strengthened linkage between thermal cycles and local properties	Emerging evidence; replication and open datasets needed

9. Research Gaps

- Thermal trajectory is rarely reported completely. Current, voltage and travel speed are often provided without time-resolved interpass temperature, dwell logic, heat-source efficiency or local cooling history.
- Heat-treatment studies use different starting microstructures and insufficiently map temperature–time–transformation behavior. Direct ageing, solution treatment and combined schedules require a common experimental baseline.

- Spatial heterogeneity is under-sampled. Bottom, middle and top locations—and parallel and transverse orientations—must be treated as planned experimental factors.
- Phase identification is sometimes based on morphology alone. Quantitative SEM–EDS/XRD should be complemented by EBSD and TEM where γ″/δ discrimination is central.
- Corrosion evidence is narrower than tensile evidence, and service-relevant combinations of stress, temperature, chloride exposure and cyclic loading are uncommon.
- Fatigue, creep, fracture toughness and crack-growth datasets remain inadequate for safety-critical qualification.
- Predictive models frequently use small, platform-specific datasets. Physics-informed and uncertainty-aware models need independent validation.
- Environmental claims need consistent system boundaries including wire production, shielding gas, heat treatment, machining allowance, rejected builds and recycling.
- Reporting standards are inconsistent, preventing reliable meta-analysis and industrial transfer.

9.1 Evidence-linked research-gap matrix

Table 7 links each observed limitation to its evidence pattern, consequence and required research response.

Table 7. Evidence-based research gaps and corresponding research responses.

Observed limitation	Evidence pattern	Academic/industrial consequence	Research response
Incomplete thermal-history reporting	Many studies report nominal current, voltage and speed but not time-resolved interpass temperature	Poor reproducibility and weak transfer between wall geometries	Calibrated pyrometry/IR monitoring, full I–V logging and validated transient models
Incompatible heat-treatment schedules	Different as-built segregation states, temperatures, times and cooling routes	No universal optimum; contradictory property trends	Matched-wall randomization, designed temperature–time matrix and phase-resolved characterization
Sparse fatigue/creep/fracture data	Evidence dominated by hardness and monotonic tensile tests	Static acceptance cannot establish damage tolerance	Orientation- and defect-resolved fatigue, crack growth, fracture and creep testing
Non-standard corrosion testing	Electrolyte, surface finish, scan rate and exposed area vary	Electrochemical values cannot be pooled reliably	Harmonised pitting, EIS, immersion, intergranular and high-temperature protocols
Small platform-specific datasets	Predictive models trained on narrow parameter windows	Uncertain extrapolation and hidden model bias	Open machine-readable datasets, uncertainty quantification and independent confirmation
Incomplete sustainability boundaries	Gas, heat treatment, machining and rejected builds often omitted	Potentially overstated environmental benefit	Cradle-to-gate sensitivity analysis linked to quality and post-processing

10. Recommended Research and Qualification Framework

Figure 2 presents the overall qualification framework proposed in this section.

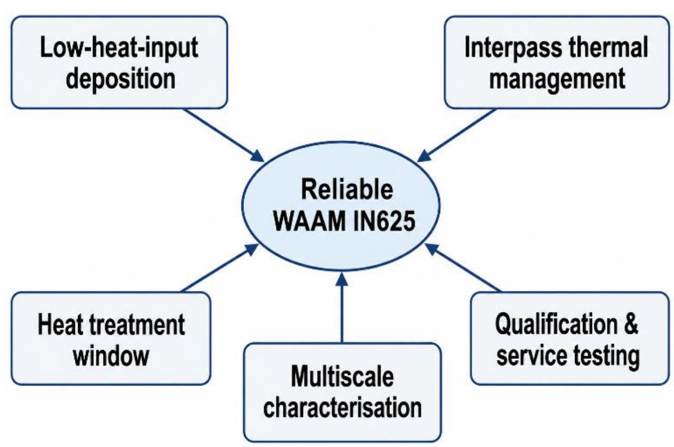

Figure 2: Integrated framework proposed for reliable WAAM processing and qualification of IN625 (authors' synthesis).

A defensible programme should begin with single-bead and multi-layer stability trials, followed by a statistically designed wall experiment. Current/voltage waveform, wire-feed rate, travel speed and controlled interpass temperature should be primary factors. Arc electrical signals, wire consumption, bead geometry and thermal histories should be logged for every build. A Box–Behnken or central-composite design can capture curvature with fewer trials than a full factorial design, but centre-point replication and confirmation runs are essential.

After identifying a stable deposition window, the wall should be divided by height and orientation. Characterization should include optical microscopy, SEM–EDS maps, XRD, EBSD texture/grain analysis, microhardness mapping and volumetric defect inspection. Heat-treatment specimens should originate from matched wall locations and be randomly assigned to as-deposited, solution-treated, directly aged and solution-plus-aged groups. Treatment variables should include temperature and holding time, with controlled cooling and recorded furnace uniformity. Table 8 specifies the minimum measurements and recommended analysis for each stage of this programme.

Table 8: Minimum experimental and reporting matrix for qualification-oriented WAAM Alloy 625 research.

Stage	Minimum measurements	Recommended analysis / output
Feedstock and substrate	Wire certificate, diameter, surface condition; substrate grade/thickness	Traceable chemistry and dilution baseline
Deposition	I–V waveform, WFR, speed, gas, CTWD, path, layer height, dwell	Net heat/mass input; stability indices; reproducibility
Thermal monitoring	Peak/interpass temperature, cooling time, spatial thermal history	Calibrated thermal model and location-specific descriptors
Geometry/defects	Bead width/height, waviness, dilution, CT/penetrant inspection	Process window and defect probability
Microstructure	OM, SEM–EDS, XRD, EBSD; TEM for nanoscale phases	Grain/texture, SDAS, segregation and phase fractions
Mechanical	Hardness map; tensile in two directions; impact/fracture; fatigue/creep as applicable	ANOVA with confidence intervals; anisotropy ratios
Environment	Polarization, EIS, immersion/oxidation; wear at service temperature	Mechanism-linked corrosion/oxidation/wear performance
Integration	Multi-response desirability or Pareto optimization; confirmation builds	Validated parameter/heat-treatment recommendation

11. Recommended Reporting Checklist

- Report power-source model, arc mode, polarity, waveform setting and measured current/voltage statistics—not nominal values alone.
- State wire heat/lot, diameter and certified composition; specify substrate grade, size and preparation.
- Provide robot/toolpath, contact-tip-to-work distance, torch angle, shielding composition/flow and environmental protection.
- Define heat-input equation and efficiency assumption; report wire mass per unit length and deposition efficiency.
- Record interpass temperature measurement location, emissivity/calibration, threshold and dwell-time distribution.
- Identify coupon coordinates, wall height, build orientation, machining direction and applicable test standard.
- Give heat-treatment temperature uniformity, hold-time origin, atmosphere and cooling rate/method.
- Report replicates, dispersion, statistical model adequacy, lack-of-fit and independent confirmation.
- Archive raw process signals, thermal histories and machine-readable property data where possible.

11.1 Limitations of the Review

This study is a critical narrative review, not a protocol-registered systematic review. Indexing differences may have excluded regional, non-English or very recent early-access papers. Experimental heterogeneity in arc source, waveform, wall geometry, feedstock lot, heat-input convention, coupon orientation, surface preparation and heat treatment prevented formal meta-analysis. Several 2026 studies were available only as early-view records, and their bibliographic details may change at issue assignment. Quantitative values are therefore interpreted conditionally and should not be used as universal design allowable. These limitations motivate the reporting framework proposed in Section 10.

12. Conclusions

RQ1—Thermal control. Strong evidence shows that the final material state is governed by the complete thermal trajectory created by arc mode, coupled heat/mass input, interpass temperature, path strategy and wall geometry. Nominal heat input alone is insufficient.

RQ2—Microstructure. Strong multi-study agreement supports a textured γ-Ni dendritic matrix with location-dependent Nb/Mo segregation and interdendritic constituents. The magnitude and service consequence of these features remain conditional on defects, texture and reheating history.

RQ3—Heat treatment. Moderate evidence shows that solution treatment can reduce segregation and dissolve Nb-rich constituents, while ageing can increase hardness or yield strength. No universal schedule is justified because grain growth, δ/γ″/carbide evolution and cooling route create competing effects.

RQ4—Qualification gaps. Strong evidence identifies inconsistent reporting and inadequate spatial sampling; moderate-to-limited evidence exists for fatigue, creep, fracture, residual stress and combined service environments. These are the principal barriers to safety-critical qualification.

RQ5—Minimum framework. Transferable results require traceable feedstock, measured process signals, temperature-triggered interpass control, location/orientation-resolved sampling, quantitative phase/texture analysis, replicated service-relevant tests, uncertainty reporting and confirmation builds.

The distinctive contribution of this review is the integration of recent Alloy 625 evidence into a condition-aware process–thermal history–microstructure–performance framework and evidence-linked research and reporting agenda. Emerging 2025–2026 approaches—including field assistance, improved thermal modelling and extended ageing studies—are promising, but require independent replication before being treated as established qualification routes.

Building directly on the gaps identified in Section 9 and the framework proposed in Section 10, the authors are undertaking planned experimental investigations aimed at improving the mechanical and metallurgical properties of Inconel 625 alloy fabricated through WAAM. That work will apply the process–thermal history–microstructure–performance framework, the evidence-based heat-treatment matrix (Table 4) and the minimum reporting protocol (Table 8) proposed here to a coordinated, single-platform experimental dataset, addressing RQ1–RQ3 with matched process and heat-treatment conditions.

Declarations

Funding: No specific funding was received for preparation of this review manuscript.

Conflict of interest: The authors declare no conflict of interest.

Data availability: No new experimental dataset was generated. The article synthesises the literature cited below.

AI-assisted writing disclosure: Generative AI tools were used to assist with literature screening, drafting support and editorial/technical verification during manuscript preparation. The authors reviewed, verified and take full responsibility for all technical content, citations and conclusions in this article.

Author contributions: Amit Kumar Punia—corresponding author; literature investigation, initial synthesis and manuscript preparation. Rakesh Kumar—conceptualisation, critical analysis, supervision and manuscript revision.

References

[1] Safarzade, A., Sharifitabar, M. and Shafiee Afarani, M. (2020), ‘Effects of heat treatment on microstructure and mechanical properties of Inconel 625 alloy fabricated by wire arc additive manufacturing process’, Transactions of Nonferrous Metals Society of China, 30. https://doi.org/10.1016/S1003-6326(20)65439-5.

[2] Ganesan, R., Murugan, N. and Ramasamy, A. (2020), ‘Microstructure and mechanical properties of Inconel-625 slab component fabricated by wire arc additive manufacturing’, Materials Science and Technology, 36, 1785–1795. https://doi.org/10.1080/02670836.2020.1836737.

[3] Jiang, Q., Zhang, P., Yu, Z., Shi, H., Li, S., Wu, D., Yan, H., Ye, X. and Chen, J. (2020), ‘Microstructure and mechanical properties of thick-walled Inconel 625 alloy manufactured by WAAM with different torch paths’, Advanced Engineering Materials. https://doi.org/10.1002/adem.202000728.

[4] Mookara, R., Seman, S., Ren, J. and Amirthalingam, M. (2021), ‘Influence of droplet transfer behaviour on the microstructure, mechanical properties and corrosion resistance of wire arc additively manufactured Inconel (IN) 625 components’, Welding in the World. https://doi.org/10.1007/s40194-020-01043-6.

[5] Votruba, V., Diviš, I., Pilsová, L., Zeman, P., Beránek, L., Horváth, J. and Smolík, J. (2022), ‘Experimental investigation of CMT discontinuous wire arc additive manufacturing of Inconel 625’, International Journal of Advanced Manufacturing Technology, 122, 711–727. https://doi.org/10.1007/s00170-022-09878-7.

[6] Akselsen, O.M., Bjørge, R., Ånes, H.W., Ren, X. and Nyhus, B. (2022), ‘Microstructure and properties of wire arc additive manufacturing of Inconel 625’, Metals, 12, 1867. https://doi.org/10.3390/met12111867.

[7] Cheepu, M.M., Lee, C. and Cho, S.-M. (2020), ‘Microstructural characteristics of wire arc additive manufacturing with Inconel 625 by super-TIG welding’, Transactions of the Indian Institute of Metals, 73, 1475–1479. https://doi.org/10.1007/s12666-020-01915-x.

[8] Sword, J.I. et al. (2024), ‘Analysis of environmental impact and mechanical properties of wire arc additively manufactured Inconel 625 impeller’, Sustainability, 16, 4178. https://doi.org/10.3390/su16104178.

[9] Xia, C., Pan, Z., Polden, J., Li, H., Xu, Y., Chen, S. and Zhang, Y. (2020), ‘A review on wire arc additive manufacturing: monitoring, control and a framework of automated system’, Journal of Manufacturing Systems, 57, 31–45. https://doi.org/10.1016/j.jmsy.2020.08.008.

[10] Guo, C., Ying, M., Dang, H., Hu, R. and Chen, F. (2021), ‘Microstructural and intergranular corrosion properties of Inconel 625 superalloys fabricated using wire arc additive manufacturing’, Materials Research Express, 8, 035103. https://doi.org/10.1088/2053-1591/abe977.

[11] Sharma, H., Singla, J., Singh, V., Singh, J., Kumar, H., Bansal, A., Singla, A.K., Goyal, D.K. and Gupta, M.K. (2023), ‘Influence of post heat treatment on metallurgical, mechanical, and corrosion analysis of wire arc additive manufactured Inconel 625’, Journal of Materials Research and Technology, 27, 5910–5923. https://doi.org/10.1016/j.jmrt.2023.11.074.

[12] Kocaman, E., Gürol, U., Günen, A. et al. (2025), ‘Effect of post-deposition heat treatments on high-temperature wear and corrosion behavior of Inconel 625’, Materials Today Communications, 42, 111101. https://doi.org/10.1016/j.mtcomm.2024.111101.

[13] Saravanakumar, K., Balaji, V.G., Srijha, T., Sanjay, V. and Thatchuneswaran, K. (2024), ‘Analysis of microstructure and mechanical properties of Inconel 625 alloy by wire arc additive manufacturing (WAAM)’, Archives of Metallurgy and Materials, 69, 1079–1086. https://doi.org/10.24425/amm.2024.150928.

[14] Wang, Y., Chen, X., Shen, Q., Su, C., Zhang, Y., Jayalakshmi, S. and Singh, R.A. (2021), ‘Effect of magnetic field on the microstructure and mechanical properties of Inconel 625 superalloy fabricated by wire arc additive manufacturing’, Journal of Manufacturing Processes, 64, 10–19. https://doi.org/10.1016/j.jmapro.2021.01.008.

[15] Kumar, A., Maji, K. and Shrivastava, A. (2023), ‘Investigations on deposition geometry and mechanical properties of wire arc additive manufactured Inconel 625’, International Journal of Precision Engineering and Manufacturing, 24, 1483–1500. https://doi.org/10.1007/s12541-023-00827-2.

[16] Xu, D., Lu, Z., Chen, L. et al. (2024), ‘Prediction of tensile properties in Inconel 625 superalloy fabricated by wire arc additive manufacturing using improved artificial neural network’, Applied Sciences, 14, 3240.

[17] Ceritbinmez, F., Günen, A., Gürol, U. et al. (2023), ‘A comparative study on drillability of Inconel 625 alloy fabricated by wire arc additive manufacturing’, Journal of Manufacturing Processes, 89, 150–169. https://doi.org/10.1016/j.jmapro.2023.01.072.

[18] Farias, F.W.C., Lira, M.N. and Payão Filho, J.C. (2026), ‘Arc-based directed energy deposited Inconel 625: aging heat treatment development’, Journal of Alloys and Compounds, 1050, 185516. https://doi.org/10.1016/j.jallcom.2025.185516.

[19] Sharifitabar, M., Khorshahian, S. et al. (2022), ‘High-temperature oxidation performance of Inconel 625 superalloy fabricated by wire arc additive manufacturing’, Corrosion Science, 197, 110087. https://doi.org/10.1016/j.corsci.2022.110087.

[20] Mukhrish, Y.E. et al. (2024), ‘Experimental investigations on wire arc additive manufacturing process using an Inconel 625 alloy wire’, Mechanics of Advanced Materials and Structures. https://doi.org/10.1080/15376494.2023.2256336.

[21] Mohanraj, R. and Abdul Basith, S.N. (2024), ‘A review on microstructure and mechanical properties of Inconel 625 alloy fabricated using wire arc additive manufacturing process’, Rapid Prototyping Journal, 30, 1337–1347. https://doi.org/10.1108/RPJ-11-2023-0387.

[22] Yu, S.P. et al. (2026), ‘Enhancing microstructure and mechanical properties of Inconel 625 by a low-cost static magnetic field-assisted WAAM process’, Welding in the World. https://doi.org/10.1007/s40194-026-02408-z.

[23] Mishra, R., Imam, M., Chinthapenta, V. and Mastanaiah, P. (2024), 'Thermo-mechanical modelling of the wire arc based additively manufactured Inconel 625 superalloy', Materials Today: Proceedings, 108, 53–64. https://doi.org/10.1016/j.matpr.2023.08.142.

[24] Banerjee, A., Souza, P., Mckegney, S., Pimentel, M., da Silva, L., King, M. and Rahimi, S. (2026), 'Near-net-shape wire-arc additive manufacturing (WAAM) of bimetallic P22 steel and Inconel 625: microstructure–property correlations', Progress in Additive Manufacturing, 11, 3125–3135. https://doi.org/10.1007/s40964-025-01511-9.

[25] Dinh, D.M., Le, V.T., Tran, V.C. and Pham, Q.H. (2026), 'An experimental–numerical investigation on thermal cycles and their effects on microstructure and mechanical properties in wire arc additive manufacturing of Inconel 625 superalloy rectangular walls', Welding in the World. https://doi.org/10.1007/s40194-026-02440-z.

[26] Tanvir, A.N.M., Ahsan, M.R.U., Seo, G., Kim, J., Ji, C., Bates, B., Lee, Y. and Kim, D.B. (2020), 'Heat treatment effects on Inconel 625 components fabricated by wire + arc additively manufacturing (WAAM)—part 2: mechanical properties', International Journal of Advanced Manufacturing Technology, 110, 1709–1721. https://doi.org/10.1007/s00170-020-05980-w.

[27] Rodrigues, T.A., Farias, F.W.C., Avila, J.A., Maawad, E., Schell, N., Santos, T.G. and Oliveira, J.P. (2023), 'Effect of heat treatments on Inconel 625 fabricated by wire and arc additive manufacturing: an in situ synchrotron X-ray diffraction analysis', Science and Technology of Welding and Joining. https://doi.org/10.1080/13621718.2023.2187927.

[28] Special Metals Corporation (technical bulletin), 'INCONEL® alloy 625: composition, properties and applications', nominal-composition reference for UNS N06625. Manufacturer data used for background specification context only.

[29] Sarathchandra, D.T. and Davidson, M.J. (2021), 'Effect of heat input on mechanical and microstructural properties of Inconel 625 depositions processed in wire arc additive manufacturing', Proceedings of the Institution of Mechanical Engineers, Part B. https://doi.org/10.1177/09544089211004718.

[30] Rosli, N.A., Alkahari, M.R., Abdollah, M.F., Maidin, S., Ramli, F.R. and Herawan, S.G. (2021), 'Review on effect of heat input for wire arc additive manufacturing process', Journal of Materials Research and Technology. https://doi.org/10.1016/j.jmrt.2021.02.002.

[31] Chaturvedi, M., Scutelnicu, E., Rusu, C.C., Mistodie, L.R., Mihailescu, D. and Subbiah, A.V. (2021), 'Wire arc additive manufacturing: review on recent findings and challenges in industrial applications and materials characterization', Metals, 11, 939. https://doi.org/10.3390/met11060939.

[32] Zhang, C., Qiu, Z., Zhu, H., Wang, Z., Muránsky, O., Ionescu, M., Pan, Z., Xi, J. and Li, H. (2022), 'On the effect of heat input and interpass temperature on the performance of Inconel 625 alloy deposited using WAAM–CMT', Metals, 12, 46. https://doi.org/10.3390/met12010046.

[33] Treutler, K. and Wesling, V. (2021), 'The current state of research of wire arc additive manufacturing (WAAM): a review', Applied Sciences, 11, 8619. https://doi.org/10.3390/app11188619.

[34] Raut, L.P. and Taiwade, R.V. (2021), 'Wire arc additive manufacturing: a comprehensive review and research directions', Journal of Materials Engineering and Performance, 30, 4768–4791.

[35] Pham, Q.H., Nguyen, V.T. and Tran, V.C. (2024), 'Wire and arc additive manufacturing of Inconel 625 and 718 alloys: microstructures, defects and improvement methods', HaUI Journal of Science and Technology, 60(5), 164–168.

[36] Paranthaman, V., Poosapadi, D., Sailesh, A., Sharma, V., Singh, R., Rajasekhara Babu, L., Arun, K.K., Ravichandran, M. and Senthil, T.S. (2025), 'Role of heat treatment in enhancing microstructure and properties of Inconel 625 manufactured by directed energy deposition using wire arc', Journal of Alloys and Metallurgical Systems, 100147. https://doi.org/10.1016/j.jalmes.2024.100147.

[37] Gurmesa, F.D. et al. (2025), 'Effects of wire diameter on mechanical and microstructural properties of wire arc additively manufactured Inconel 625', Journal of Materials Research and Technology (2025).

[38] Krishnasamy, S. et al. (2025), 'Heat treatment effects on the top and bottom zones of a GTAW-WAAM Inconel 625 multilayer wall', Strojniški vestnik—Journal of Mechanical Engineering (2025).

[39] Singla, J., Singh, J., Singh, V. and Rooprai, R.S. (2025), 'Influence of post heat treatment on slurry erosion behavior of wire arc additive manufactured Inconel-625', Key Engineering Materials, 1010, 65–72.

[40] Patel, D. et al. (2025), 'A review on wire arc additive manufacturing of Inconel alloys', Engineering Proceedings, 114, 6.

[41] Yin, X., He, G., Meng, W. et al. (2020), 'Comparison study of low-heat-input wire-arc-fabricated nickel-based alloy by cold metal transfer and plasma arc', Journal of Materials Engineering and Performance, 29, 4222–4232.

[42] Chintala, A., Kumar, M.T., Sathishkumar, M., Arivazhagan, N. and Manikandan, M. (2021), 'Technology development for producing Inconel 625 in aerospace application using wire arc additive manufacturing', Journal of Materials Engineering and Performance, 30, 5333–5341. https://doi.org/10.1007/s11665-021-05781-6.

Cite this article as: Amit Kumar Punia, Rakesh Kumar, Arvind Jayant, Wire arc additive manufacturing of Inconel 625: A Review, International Journal of Research in Engineering and Innovation, 10 (5), (2026), 185-195.
https://doi.org/10.36037/IJREI.2026.10501